ACS APPLIED MATERIALS & INTERFACES

Research Article

www.acsami.org

Fundamental Study of Electrospun Pyrene–Polyethersulfone Nanofibers Using Mixed Solvents for Sensitive and Selective Explosives Detection in Aqueous Solution

Xiangcheng Sun,[†] Yixin Liu,[†] George Shaw,[†] Andrew Carrier,[†] Swayandipta Dey,[‡] Jing Zhao,[‡] and Yu Lei*[,†]

[†]Department of Chemical and Biomoleclular Engineering, and [‡]Department of Chemistry, University of Connecticut, Storrs, Connecticut 06269, United States

Supporting Information

ABSTRACT: Fluorescent pyrene–polyethersulfone (Py–PES) nanofibers were prepared through electrospinning technique using mixed solvents. The effects of mixed solvent ratio and polymer/fluorophore concentrations on electrospun nanofiber's morphology and its sensing performance were systematically investigated and optimized. The Py–PES nanofibers prepared under optimized conditions were further applied for highly sensitive detection of explosives, such as picric acid (PA), 2,4,6-trinitrotoluene (TNT), 2,4-dinitrotoluene (DNT), and 1,3,5-trinitroperhydro-1,3,5-triazine (RDX) in aqueous phase with limits of detection ($S/N = 3$) of 23, 160, 400, and 980 nM, respectively. The Stern–Volmer (S–V) plot for Py excimer fluorescence quenching by PA shows two linear regions at low (0–1 μM) and high concentration range (>1 μM) with a quenching constant of 1.263×10^6 M^{-1} and 5.08×10^4 M^{-1}, respectively. On the contrary, S–V plots for Py excimer fluorescence quenching by TNT, DNT, and RDX display an overall linearity in the entire tested concentration range. The fluorescence quenching by PA can be attributed to the fact that both photoinduced electron transfer and energy transfer are involved in the quenching process. In addition, pyrene monomer fluorescence is also quenched and exhibits different trends for different explosives. Fluorescence lifetime studies have revealed a dominant static quenching mechanism of the current fluorescent sensors for explosives in aqueous solution. Selectivity study demonstrates that common interferents have an insignificant effect on the emission intensity of the fluorescent nanofibers in aqueous phase, while reusability study indicates that the fluorescent nanofibers can be regenerated. Spiked real river water sample was also tested, and negligible matrix effect on explosives detection was observed. This research provides new insights into the development of fluorescent explosive sensor with high performance.

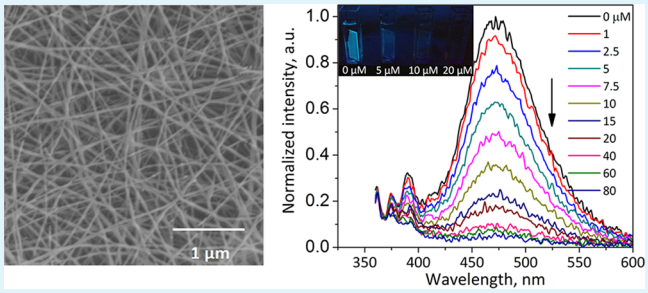

KEYWORDS: *electrospun nanofibers, mixed solvents, fluorescence quenching, explosives detection, aqueous phase, sensing mechanism*

INTRODUCTION

Given the extensive applications of explosives in mass-destruction weapons as well as their environmental toxicity, explosive detection has attracted great research interest over the past few decades.[1−3] Current explosive detection methods either use canines or heavily rely on sophisticated instruments that are expensive, complex, and lack portability.[4,5] Therefore, there is an urgent need to develop low-cost, simple, and field-applicable explosive detectors with high performance. In this regard, fluorescent sensors are particularly attractive because of their sensitivity, selectivity, short response time, simplicity, and low cost.[4,6] Fluorescent conjugated polymers (CPs) have been extensively explored as fluorescent active sensing materials in explosive detection because of their amplified response and improved sensitivity.[7−9] Swager and co-workers pioneered a conjugated polymer scaffold and achieved unprecedented sensitivity and selectivity for TNT.[10,11] Trogler group developed a new class of fluorescent films that were prepared by spin-coating of inorganic polymers onto solid substrates for detecting nitroaromatic explosives.[12] Recently, oligofluorophore based xerogel fibers or nanoparticles have also been developed and applied as explosives sensors with ultrasensitivity to nitro explosives.[13−16]

Although these sensors exhibited sensitive response to nitroaromatic compounds (NACs), they may suffer from the short lifetime and/or sacrifice on the sensing performance when applied to aqueous samples.[17−19] In many occasions, explosive detection is required to be performed in aqueous matrix. For example, sensing of NACs in groundwater or seawater is critical for detecting buried unexploded ordnance, for locating underwater mines, as well as for characterizing soil and groundwater contaminated by toxic TNT at military

Received: November 13, 2014
Accepted: June 1, 2015
Published: June 1, 2015

DOI: 10.1021/acsami.5b03655
ACS Appl. Mater. Interfaces 2015, 7, 13189−13197

bases.[20,21] Recently, our group reported the use of small fluorophore such as pyrene doped in polymer as explosive sensing materials.[6,22,23] Similar research was also reported by Bayindir and co-workers, where they observed fast and sensitive detection of explosive vapors through pyrene doped polyethersulfone thin films.[5] The pyrene doped polymer films demonstrated fast and sensitive fluorescence quenching to NACs vapors. However, its application for explosive detection in aqueous solution has not been explored much. Furthermore, the quenching mechanism, whether it is static/dynamic or both, has not been fully investigated in these studies either.

Electrospinning is a well-known versatile method for generating nanofibers with a diameter in the range of 10−1000 nm.[24,25] This technique has proven to be a unique and cost-effective approach to generate nanofibrous films with high porosity and large surface area approximately 1−2 orders of magnitude more than that of the continuous thin film,[22,26,27] which favors the development of chemical sensors with high sensitivity and fast response. It is well-known that polymer concentration plays a crucial role in electrospinning process. Hsiao et al. reported that when polyethersulfone (PES) concentration decreased, beads formed within the scaffold through electrospinning process.[28] This is a common phenomenon occurred during electrospinning process when polymer concentration is below their entanglement concentration or when the viscoelasticity of the nanofibers favors bead formation. In general, low polymer concentration favors the formation of nanofibers with smaller diameters,[25] which is favorable for fluorescence sensing application. In this regard, to electrospin small nanofibers using polymer concentration as low as possible is necessary in order to realize explosive fluorescent detection with high performance. In addition, the change of polymer concentrations affects polymer/fluorophore ratio and tunes the electronic structure of fluorophore doped in polymer, thus further affecting the fluorescence quenching performance of the nanofibrous film.[6]

In this work, pyrene doped PES (Py−PES) nanofibers were electrospun using mixed solvents and relatively low polymer concentration for the first time. The effects of the ratio of mixed solvents and the concentrations of polymer and fluorophore on nanofiber morphology and quenching performance were studied systematically. The electrospun Py−PES nanofibers with desired morphology and best quenching performance were then employed as fluorescent sensors for detecting traces of explosives including picric acid (PA), 2,4,6-trinitrotoluene (TNT), 2,4-dinitrotoluene (DNT), and 1,3,5-trinitroperhydro-1,3,5-triazine (RDX) in aqueous medium. Both good sensitivity and selectivity were achieved. The sensing mechanism was further determined based on fluorescence lifetime measurements of the sensing film in the absence and presence of explosives. This study provides new insights into the development of fluorescent explosive sensors with high performance.

EXPERIMENTAL SECTION

Materials. The polymer polyethersulfone (PES, Radel, H-3000, Mw = 780 000 g/mol) was provided by Solvay Advanced Polymers. Tetrahydrofuran (THF, ≥99.0%), *N*,*N*-dimethylformamide (DMF, anhydrous, 99.8%), tetrabutylammonium hexafluorophosphate (NBu_4PF_6, 98%), 2,4-dinitrotoluene (DNT, 97%), and picric acid (PA) were purchased from Sigma-Aldrich. Pyrene (98%) was bought from Acros Organics. 2,4,6-Trinitrotoluene (TNT) was purchased from Ultra Scientific, while 1,3,5-trinitroperhydro-1,3,5-triazine (RDX) was obtained from Chem Service. All chemicals used in the experiments were of analytical reagent grade. The real water sample was obtained from a river in Willimantic, CT, USA.

Solution Preparation. Appropriate amounts of PES were dissolved in DMF followed by the addition of THF in order to obtain the desired concentrations in mixed DMF/THF solvents with different volume ratios (DMF/THF = 10/0, 7/3, 6/4, 5/5, 4/6, 3/7, respectively). All prepared solutions also contain 0.1 M pyrene and 2 wt % of NBu_4PF_6, endowing the fluorescence and increasing the conductivity of polymer solution, respectively, as used in our previous study.[22,23]

Electrospinning. The nanofibers were generated by electrospinning with a flow rate of 0.3 mL/h at an applied voltage of 25 kV over a collection distance of 10 cm. All the experiments were performed at 25 °C. The electrospun nanofibers are denoted as Py−PES nanofibers. During electrospinning process, mixed solvent (THF/DMF) evaporates, thus leaving dry Py−PES nanofibers on the collector.

Characterization. The viscosity of polymer solutions was measured by an AR G2 rheometer. The morphology of the fluorescent films was obtained using JEOL 6335F field emission scanning electron microscope (SEM) at an acceleration voltage of 10 kV, and the average diameters of electrospun nanofibers were measured from 50 randomly selected nanofibers in the SEM images using ImageJ software. The absorption spectra of Py−PES films were obtained using a Cary 50 UV−vis spectrophotometer (Agilent Technologies).

Fluorescence Quenching Experiment. The fluorescence quenching experiments were performed similar to the literature reports.[29,30] Briefly, for explosive detection in aqueous phase, the nanofibrous film on the glass slide was inserted into the cuvette with 3 mL of distilled water, and then the solution of nitro explosives or interferents were injected and allowed to reach equilibrium before recording the fluorescence signal.[30,31] In order to study the matrix effects of real water on the current film sensor performance, fluorescence quenching experiments were also conducted in a similar way except using 3 mL of real water instead of DI water. Fluorescence emission spectra were measured through a Varian Cary Eclipse fluorescence spectrometer (Agilent Technologies), and the spectra were recorded in the range of 360−600 nm with an excitation wavelength of 344 nm. The quenching efficiency is defined as $(I_0 - I)/I_0$, where I_0 and I are the fluorescent intensity of the pyrene excimer peak (or monomer peak) in the absence and presence of explosives in the aqueous medium.

Fluorescence Lifetime Experiment. For fluorescence lifetime measurements, the nanofibrous film with different concentrations of explosives was excited with a pulse diode laser (PicoQuant) at 405 nm with a repetition rate of 2.5 MHz and a pulse width of ∼40 ps. The emission of the samples was collected with an avalanche photodiode detector (PicoQuant) using a 450 nm long-pass spectral filter in order to study the pyrene excimer photoluminescence decay. The fluorescence decay was recorded using a time-correlated single photon counting module (Picoharp 300, PicoQuant). The measurements were conducted on at least three spots for each sample.

RESULTS AND DISCUSSION

Optimization of Py−PES Nanofiber Fabrication. In this study, PES was used as the polymer matrix because of its better hydrophilicity compared with other polymers such as polystyrene used in our previous report.[22,23] For fluorescence sensing application, porous nanofibers that allow fast diffusion of analytes are highly desired. In order to prepare electrospun nanofibers, a solution with an appropriate polymer concentration or viscosity is required to obtain uniform ejection of the charged jet during electrospinning process, since extensive molecular entanglements are prerequisites for the formation of a stable and continuous charged jet. If the concentration of the solution is too low, a continuous stream of the charged jet cannot be formed, as the charged jet experiences instability leading to the formation of droplets (electrospraying). PES in

DOI: 10.1021/acsami.5b03655
ACS Appl. Mater. Interfaces 2015, 7, 13189−13197

pure solvent such as DMF can only be electrospun at relatively high concentration. Hsial et al. found that when PES concentration was lower than 20 wt %, its electrospinnability decreased and beads began to form.[28] In parallel, Fong et al. observed similar phenomenon and attributed the formation of beads to the low viscosity and high surface tension of the solutions.[32]

We found that electrospinning of Py−PES solution with PES concentration lower than 10% using DMF as sole solvent only resulted in the formation of Py−PES beads and particles instead of nanofibers, possibly because of the low viscosity of the polymer solution. With the increase of PES concentration to 20%, Py−PES nanofibers with large diameter (180.5 ± 63.4 nm) formed (see Figure S1 in the Supporting Information). However, nanofibers with large diameter are not favorable for the analyte diffusion, resulting in low sensitivity in general.

Solvent can significantly affect the electrospinnability of a polymer solution; therefore, the selection of suitable solvents is a crucial step in a successful electrospinning process.[33,34] Mixed solvents have often been applied in the electrospinning process[35] because the introduction of nonsolvent to good solvent of polymers as mixed solvents is able to control the morphology of electrospun nanofibers, at varying mixed solvent ratios.[36,37] In our case, PES can be dissolved in DMF, while it cannot be dissolved in THF. With an increase of the ratios of THF to DMF in Py−PES solution, the nanofibers can be electrospun with low probability of bead formation. Specifically, when THF was added to the Py−PES/DMF solution, the viscosity of the solution was increased. Viscosity of the polymer solution varied with the position of solvent in the given polymer solubility region because the quality of solvent−polymer interactions affects the chain geometry of the polymer.[38] Supaphol et al. observed that the addition of a cosolvent helped suppress the bead formation likely because of the increase in the viscosity and/or the conductivity of the resulting solutions.[39] In this study, the viscosities of the as-prepared Py−PES solutions with different THF to DMF ratios were measured. To our delight, we found that viscosity indeed increased with increasing ratio of THF in solvents (see Table S1 in the Supporting Information), which favors the electrospinning of nanofibers. In addition, it has been reported that increasing evaporation rate also promotes the formation of nanofibers during the electrospinning process.[40,41] As THF has a lower boiling point and a higher evaporation rate than that of DMF, the increase of its ratio in mixed solvents can speed up the evaporation rate during electrospinning process and thus promote the formation of nanofibrous mats.

To obtain nanofiber sensing films with the desired morphology, the effects of different ratios of DMF/THF (10/0, 7/3, 6/4, 5/5, 4/6, 3/7) on nanofiber morphology and quenching efficiency were investigated first by fixing PES concentration and pyrene concentration at 6 w/v % and 0.1 M, respectively. With increase of THF ratio, Py−PES nanofibers were formed gradually. The SEM images of the as-prepared Py−PES nanofibers using mixed solvents (DMF/THF = 6/4, 5/5, 4/6, 3/7) are shown in Figure 1. The "bead-on-string" morphology can be observed for the nanofibers electrospun from mixed solvent of 60% DMF and 40% of THF (DMF/THF = 6/4). When the THF ratio is further increased, better electrospinnability can be achieved and beadless nanofibers are formed (Figure 1b−d). The nanofibers become more uniform with increasing THF ratio. When DMF only or DMF/THF at a ratio of 7/3 or a higher value was used to electrospin the Py−PES solution, no nanofiber can be formed (data not shown).

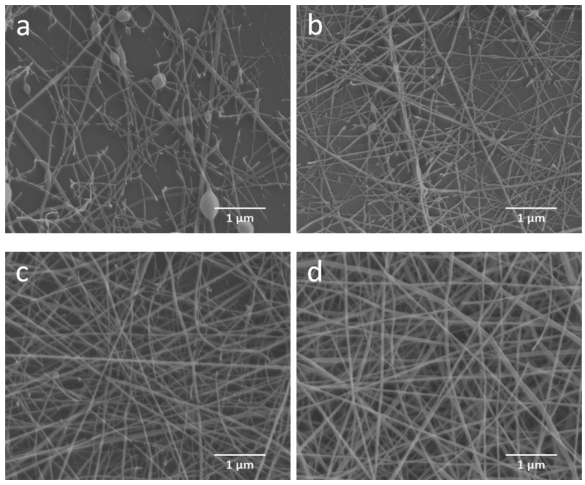

Figure 1. SEM images of nanofibrous film using 6% (w/v) PES + 0.1 M Py with different solvent ratios (DMF/THF): (a) 6/4, (b) 5/5, (c) 4/6, and (d) 3/7.

To investigate the effect of the mixed solvent ratio on the quenching efficiency of the sensing film upon exposure to 80 μM TNT solution, time-dependent fluorescence quenching studies were conducted on the four films prepared in Figure 1. The corresponding results are presented in Figure 2. Upon exposure to TNT solution, all the film sensors respond rapidly, which can be ascribed to the porous structure of nanofibrous film. After 6 min, the quenching efficiencies almost reach equilibrium, regardless of the ratios of DMF/THF. This result indicates that electronic structure determined by polymer/fluorophore ratio might play a more important role in explosive-based fluorescence quenching. Therefore, DMF/THF ratio of 4/6 was selected for subsequent experiments, as it results in the formation of nanofibers with the best morphology.

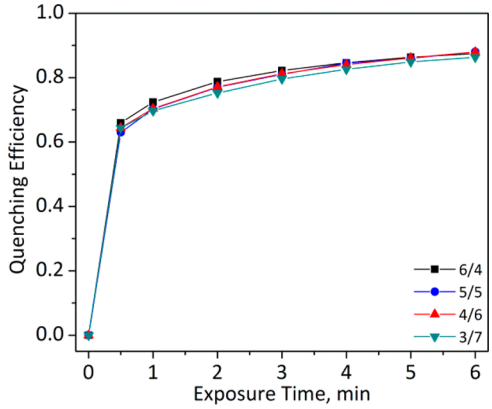

Figure 2. Time-dependent fluorescence quenching profiles were obtained for Py−PES nanofiber films electrospun from 6% PES + 0.1 M Py in mixed solvents with different ratios (DMF/THF = 6/4, 5/5, 4/6, 3/7) upon exposure to 80 μM TNT solution.

In order to study the effect of PES concentration on the nanofiber morphology as well as its quenching efficiency, experiments were carried out at a fixed Py concentration of 0.1 M and DMF/THF ratio of 4/6. Figure 3 shows the morphology of the as-prepared Py−PES nanofibers using

DOI: 10.1021/acsami.5b03655
ACS Appl. Mater. Interfaces 2015, 7, 13189−13197

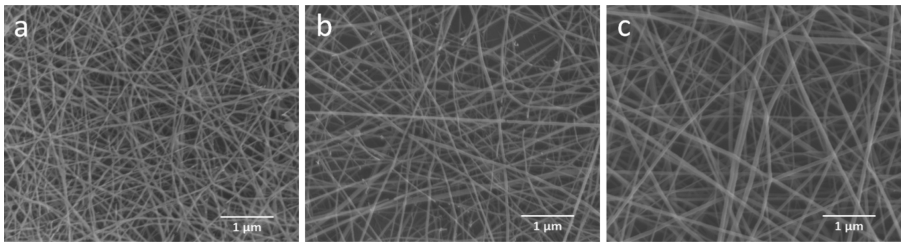

Figure 3. SEM images of nanofibrous films prepared using various PES concentrations at a fixed Py concentration of 0.1 M and DMF/THF ratio of 4/6: (a) 4%, (b) 6%, and (c) 8%.

different PES concentrations (4, 6, and 8 w/v %). When using 2% PES, only Py–PES beads/particles were observed (data not shown), which may be due to the low viscosity of the solution. With the increase of PES concentration, the diameter of Py–PES nanofibers increases as expected. The calculated average diameters for Py–PES nanofibers using 4%, 6%, and 8% PES are 37.2 ± 12.3, 44.2 ± 15.9, and 55.5 ± 21.2 nm, respectively.

The as-prepared nanofibrous films in Figure 3 were also investigated for their quenching efficiency upon exposure to 80 μM TNT solution. The response of the film sensor to TNT analyte is almost instantaneous, and it takes about 6 min to reach equilibrium (Figure 4). One can see that the quenching efficiencies for Py–PES nanofiber films prepared with PES concentration varying from 4%, 6%, and 8% were 95%, 81%, and 38%, respectively, after a 3 min exposure to 80 μM TNT solution, showing that the 4% PES generated the best sensing film. Furthermore, pyrene concentrations also affect the quenching efficiencies to explosive detection as well as nanofiber morphology (see Figures S2 and S3 in the Supporting Information). It was observed that at a fixed 4% PES and DMF/THF of 4/6, the nanofibrous film prepared using 0.1 M Py had the best quenching efficiency upon exposure to 80 μM TNT solution.

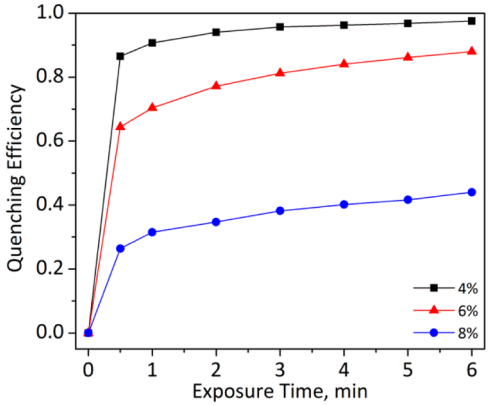

Figure 4. Time-dependent fluorescence quenching profiles were obtained for Py–PES nanofiber films electrospun from 0.1 M Py with different concentrations of PES dissolved in mixed solvents (DMF/THF = 4/6) upon exposure to 80 μM TNT solution.

The concentrations of both polymer and the doped fluorophore impact fluorescence quenching to explosives, which may be attributed to the different electronic structures resulting from different ratios of polymer to pyrene.[6] Beyazkilic et al. have shown that the polymer acts as a geometrical barrier against the dissociation of pyrene dimers and thus greatly influences the formation of pyrene excimers.[42] It is presumably believed that a sandwich-like conformation is formed between Py and PES.[5] This conformation results from the insertion of pyrene units into and between the phenyl groups, thus forming extended conjugation of π electrons and efficient long-range energy migration. This conformation also enables effective cofacial π–π stacking and affects the formation of pyrene excimers,[6] which is corroborated by various ratios of pyrene excimer to monomer emission peak value of fluorescent film with various PES concentrations (as shown in Figure S4 in the Supporting Information). From the above experiments, we found a solution consisting of 4% PES, and 0.1 M Py dissolved in DMF/THF mixed solvent (40% DMF and 60% THF) yielded the electrospun film with the best fluorescence quenching performance. Then it was used to prepare electrospun nanofibrous film for subsequent experiments. The

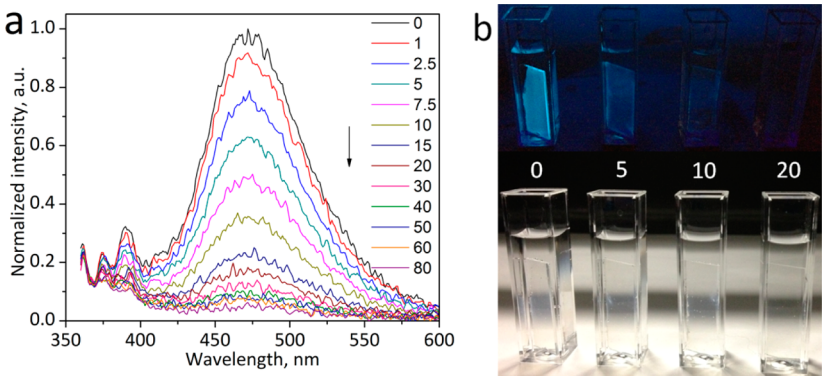

Figure 5. (a) Concentration-dependent fluorescence quenching of Py–PES nanofiber film upon the addition of different concentrations (μM) of TNT in DI water. (b) Photographs of Py–PES fluorescent nanofiber films in cuvette under UV light (254 nm, upper panel) and visible light (bottom panel) in the presence of various TNT concentrations (0, 5, 10, and 20 μM).

DOI: 10.1021/acsami.5b03655
ACS Appl. Mater. Interfaces 2015, 7, 13189–13197

absorption spectrum of the Py–PES nanofiber film was also obtained and shown in Figure S5 in the Supporting Information. The absorption spectrum of Py–PES films showed the characteristic bands at about 327 and 343 nm, corresponding to the vibrational bands of the $S_0 \rightarrow S_2$ transition of pyrene ring, which is consistent with our previous report.[6]

Nitro-Explosives Detection in Aqueous Phase. Compared with most of the reported explosive sensors for aqueous applications, fluorescent film sensors are organic-solvent-free, reusable, and convenient to use, thus providing an environment- and user-friendly detection method.[31] However, fluorophore leakage could be a potential issue in the detection of explosives in solution.[42] Therefore, the stability of pyrene entrapped in fluorescent film was investigated by monitoring the fluorescence emission of the film as well as the solution after immersion of the Py–PES nanofiber film in aqueous solution for 48 h. No obvious emission intensity difference of the fluorescent sensing film and no detectable pyrene emission from the solution were observed (the experimental details and results are illustrated in the Supporting Information as Figure S6 and S7), indicating that doped pyrene is stable in PES and the potential leakage issue is negligible for the current Py–PES nanofiber-based sensor.

To explore the ability of the as-prepared fluorescent nanofibrous film in sensing trace amounts of nitro explosives, fluorescence quenching titrations were first performed with an incremental addition of TNT to the aqueous solution. Figure 5a shows the emission spectra of Py–PES film with incremental increasing of TNT concentrations. The fluorescence intensity progressively decreases with an increase of TNT concentrations. No new emission band was observed, even at very high TNT concentrations, indicating that no new fluorescent compound was formed during the quenching experiment. Figure 5b illustrates the optical images of fluorescent nanofibrous film under 254 nm UV lamp in various concentrations of TNT aqueous solutions. Under UV light, the visible blue emission of fluorescent nanofibrous film, which was inserted in a cuvette filled with water, can be observed. With increase of TNT concentrations (from left to right), the blue emission became significantly dimmer. The obvious fluorescence change indicates that the sensor can potentially function as a naked-eye-based portable explosive sensor for aqueous samples.

The fluorescence quenching titrations with other explosive analytes (e.g., PA, DNT, and RDX) were also investigated. For these nitro explosives, strong fluorescence quenching has also been observed. The quenching behavior is characterized by the normalized fluorescence intensity (I_0/I) and quenching constant (K_{SV}) using the Stern–Volmer (S–V) equation:[8]

$$I_0/I = K_{SV}[A] + 1 \quad (1)$$

where I_0 is the initial fluorescence intensity in the absence of analytes, I is the fluorescence intensity in the presence of explosive analytes, [A] is the molar concentration of the analytes, and K_{SV} is the quenching constant (M^{-1}). Figure 6 shows the plots of I_0/I for pyrene excimer peak at ~470 nm versus the concentration of various explosives (PA, TNT, DNT, and RDX).

For the four tested explosives, their Stern–Volmer plots and the calculated quenching constants are different. The Stern–Volmer plot for PA shows two linear regions at low (0–1 μM) and high concentration (>1 μM) ranges, respectively. The observed nonlinearity over the whole PA concentration range

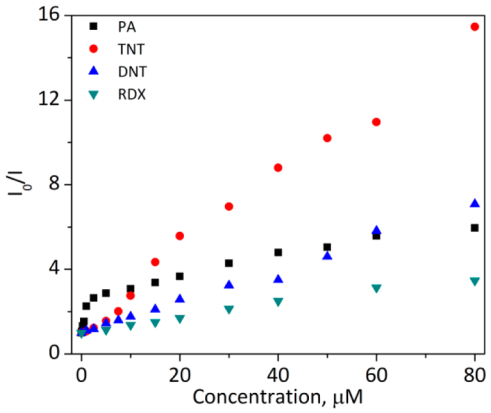

Figure 6. Stern–Volmer plots (at pyrene excimer peaks of ~470 nm) for Py–PES nanofiber film sensor upon exposure to various explosives solutions.

can be potentially attributed to energy transfer and/or self-absorption processes discussed in a later section.[4,43] Specifically the quenching constant for PA in the low concentration range is 1.263×10^6 M^{-1}, which is one of the highest values among the reported fluorescent PA aqueous sensors.[4,21,29,44] S–V plots for TNT, DNT, and RDX show almost linearity through the entire tested concentration range (see Table S2 in the Supporting Information). The quenching constants are calculated to be 1.80×10^5 M^{-1}, 7.52×10^4 M^{-1}, and 3.26×10^4 M^{-1} for TNT, DNT, and RDX, respectively. These large K_{SV} values indicate that the as-prepared fluorescent nanofibrous film is sensitive to nitro explosives in aqueous solutions and the limits of detection (LOD, calculated by using signal-to-noise ratio of 3) for PA, TNT, DNT, and RDX in aqueous solution are determined to be 23, 160, 400, and 980 nM, respectively.

Pyrene monomer emission (~393 nm) was also quenched in the presence of different explosives (Figure 7) but with much

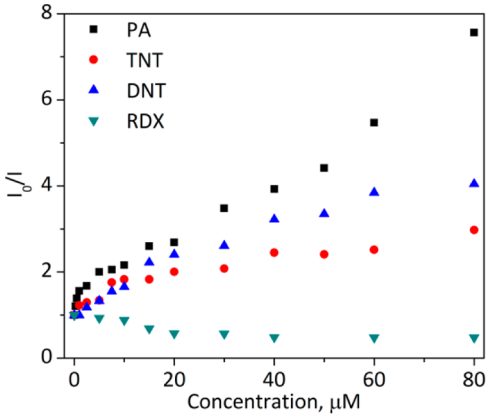

Figure 7. Stern–Volmer plots (at pyrene monomer peak of ~393 nm) for Py–PES fluorescent nanofibers film sensor with the various nitro-based explosives.

less sensitivity. Similar observations have been reported previously.[29,45,46] The calculated quenching constants in low concentration range for the monomer peak are descending in the order of PA > DNT > TNT > RDX. The order of observed quenching efficiency is not fully consistent with the LUMO energies of these compounds and the corresponding driving forces (see Table S3 and Scheme S1 in the Supporting Information). This indicates that photoinduced electron

DOI: 10.1021/acsami.5b03655
ACS Appl. Mater. Interfaces 2015, 7, 13189–13197

transfer (PET) is dominant but not the sole mechanism for the observed fluorescence quenching at monomer emission.

Sensing Mechanism for Explosives Detection. PET plays a key role in explosive quenching process due to the electron-deficient property of explosives. When excited pyrene is exposed to nitro explosives, the excited electron is transferred from the fluorophore to the explosives. The main driving force for PET process is the difference between the conduction band of the fluorescent film and the LUMO values of explosives. The LUMO orbital energy typically indicates how easily an electron can be transferred from excited fluorophore to the electron-deficient analytes. As the LUMO orbital energies of PA, TNT, DNT, and RDX calculated by density functional theory at the B3LYP/6-31G* level are in ascending energy order (see Table S3 and Scheme S1 in the Supporting Information), the order of the pyrene excimer quenching constant and sensitivity through pyrene excimer quenching is in accordance with the driving force for PET process.

Energy transfer may also occur between fluorophore and analyte, if the fluorophore and the analyte are close to each other and the analyte absorption band effectively overlaps with the fluorophore emission band, known as Förster resonance energy transfer (FRET). To examine whether FRET process occurs in our system and is responsible for the different quenching efficiencies of excimer and monomer emission for various explosives, the absorption spectra of various explosives and the emission spectrum of Py–PES nanofibrous film are recorded and presented in Figure 8.

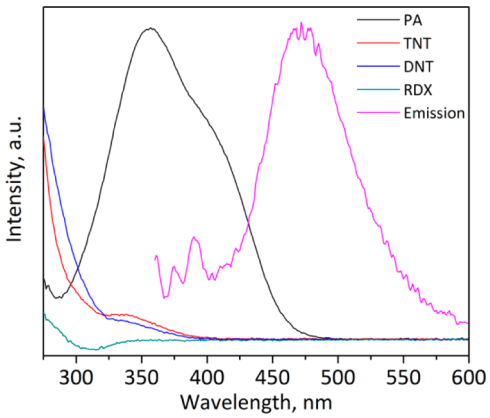

Figure 8. Absorption spectra of various explosive analytes and the emission spectrum of Py–PES nanofibrous film in DI water.

As shown in Figure 8, the Py excimer peak at ~470 nm has a small overlap with absorption of PA, but there is almost no overlap with the absorption spectra of TNT, DNT, and RDX. Therefore, both energy transfer and electron transfer mechanisms contribute to the excimer peak quenching for PA, while only electron transfer mechanism contributes to the observed quenching for other explosives. S–V plot for pyrene excimer quenching by PA shows two linear regions and bends downward at higher concentrations, which is consistent with other reports about the presence of energy transfer in fluorescence detection.[4,43] The observed bending downward of S–V plot might be attributed to the fact that some of the fluorophores are less accessible than others.[47,48]

However, in the monomer peak region, there is an overlap between absorption spectrum of PA, DNT, or TNT and the emission spectrum of Py–PES nanofibers film; thus, for all these three explosive analytes, the nonlinearity of S–V plots (Figure 7) can be observed and attributed to the presence of energy transfer. The overlap of analyte absorption and pyrene monomer emission was much larger for PA than for other explosives (e.g., DNT and TNT) in the range of 370–400 nm. The larger is the spectral overlap between the absorbance spectrum of the analyte and the emission spectrum of fluorescent film, the higher is the energy transfer efficiency and hence the stronger is the fluorescence quenching. This result is consistent with the observed good quenching performance for PA at both excimer and monomer peaks of pyrene. However, all tested explosives display a certain amount of absorption in the region of 300–370 nm; therefore, the effect of self-absorption on fluorescence quenching cannot be ruled out.

In order to further elucidate the detection mechanism of the present fluorescent sensors, the fluorescence lifetime of Py–PES nanofibrous film was measured. Normalized time-dependent fluorescence decay data with various concentrations of TNT are shown in Figure 9. The fluorescence lifetimes were

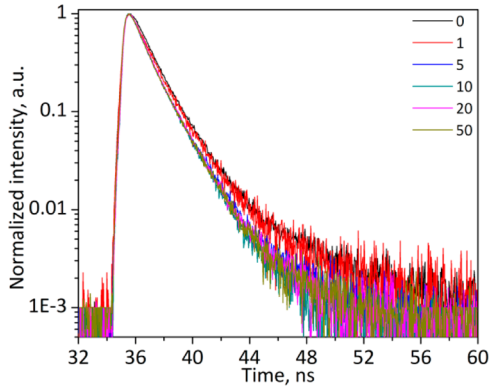

Figure 9. Normalized time-dependent fluorescence decay data of Py–PES film upon addition of TNT solutions in DI water at the following concentrations: 0, 1, 5, 10, 20, and 50 μM.

calculated by fitting the time-dependent fluorescence decay data to a single-exponential decay using the equation

$$I_{(t)} = I_{(0)} \exp\left(-\frac{t}{\tau}\right) + C \quad (2)$$

where, $I_{(t)}$ is the fluorescence intensity at time (t), $I_{(0)}$ is the initial fluorescence intensity, and τ is the fluorescence lifetime. The TNT explosive concentrations only show negligible variation in fluorescence decays of the Py–PES nanofiber films (Figure 9), although the fluorescence intensity/yield is greatly decreased by TNT solution (Figure 6). The insignificant variation in the lifetimes upon addition of explosives reveals that a static quenching mechanism might be dominant where a nonfluorescent complex forms between pyrene and explosives in the ground state Py excimer. The findings herein are consistent with that of conjugated polymer sensors and assembled monolayers of small fluorophores.[21,31,49,50] Additionally, using the S–V equation,[47,51,52] $I_0/I = k_q\tau_0[A] + 1 = K_{SV}[A] + 1$, where k_q is the bimolecular quenching constant and τ_0 is the fluorophore lifetime in the absence of quencher. k_q was calculated to be 1.03×10^{14} M^{-1} s^{-1}, which is much larger than the value of 10^{10} M^{-1} s^{-1} for a conventional diffusion quenching process. This result further supports the claim that

DOI: 10.1021/acsami.5b03655
ACS Appl. Mater. Interfaces 2015, 7, 13189–13197

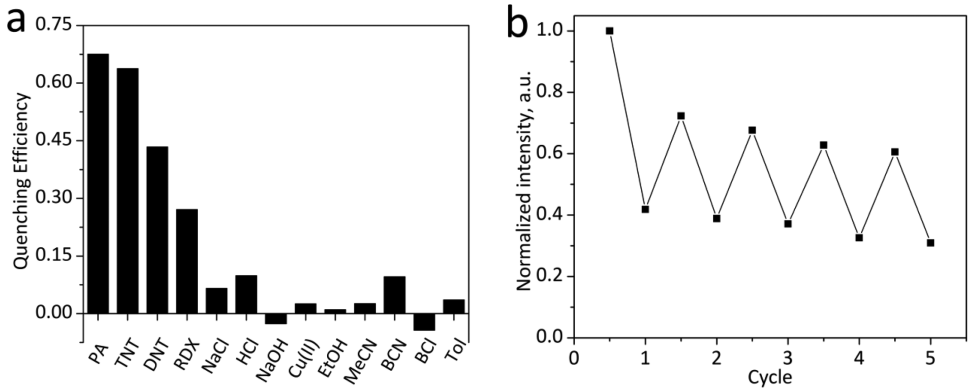

Figure 10. (a) Quenching efficiencies ($\lambda_{em} \approx 470$ nm) of Py–PES films for 10 μM nitro explosives and various interferents (such as ethanol (EtOH), acetonitrile (MeCN), benzonitrile (BCN), chlorobenzene (BCl), and toluene (Tol)) in DI water at room temperature. (b) Reusability study for the Py–PES film, where the fluorescence intensity of the Py–PES film in DI water and TNT solution (10 μM) was recorded alternatively ($\lambda_{em} \approx 470$ nm).

the static quenching process might be dominant in the Py–PES sensors.

Selectivity and Reusability of the Sensor. Good selectivity and reusability are two crucial criteria for the practical use of any sensing material. To test the selectivity of the Py–PES sensor, the fluorescence intensity of electrospun Py–PES nanofibrous film exposed to various analytes at 10 μM was monitored, and the corresponding quenching efficiencies (Py excimer) are presented in Figure 10a. One can see that commonly used chemicals including inorganic salts, acid, alkali, metal ions, organic solvents, such as ethanol (EtOH), acetonitrile (MeCN), benzonitrile (BCN), chlorobenzene (BCl), and toluene (Tol), show insignificant effect on the measured fluorescent intensity. These results suggest that the fluorescent Py–PES nanofibrous film is highly selective for explosives detection. Furthermore, we examined the regeneration of fluorescence signal (pyrene excimer peak) of a Py–PES film after it was quenched in 10 μM TNT aqueous solution (Figure 10b). In order to recover the fluorescence signal, the film was simply immersed in water and then dried in air. The rinsed film was reused to detect 10 μM TNT, and the whole process was repeated multiple times. Although the fluorescence of the sensing film cannot be fully regenerated to its original state because of incomplete removal of TNT from pyrene (caused by their strong interaction), the normalized fluorescence change is similar except for the first cycle, indicating that Py–PES film is reusable for explosive detection.

Detection of Nitro Explosives in Real Water Sample. Figure 11 depicts the comparison of the quenching efficiencies of various nitro explosives at 10 μM to the fluorescence emission of Py–PES nanofibrous film in DI water and in spiked real river water sample (Willimantic, CT). As expected, the quenching efficiencies of nitro explosives in DI water and real water are nearly overlapped, and the differences are less than 7% for all the nitro explosives. One can see that the matrix effect of real river water is negligible. This result indicates that the as-prepared explosive sensing film is a good candidate for real application.

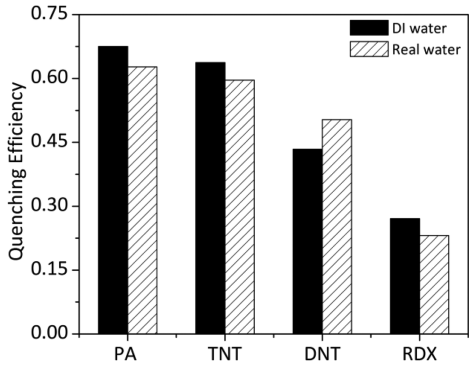

Figure 11. Quenching efficiencies ($\lambda_{em} \approx 470$ nm) of Py–PES films for various nitro explosives (10 μM) in DI water and real water sample.

CONCLUSION

Py–PES nanofibers have been electrospun using mixed solvents. Effects of the mixed solvent ratio and polymer/fluorophore concentrations on the morphology and the sensitivity of fluorescent films upon exposure to TNT solution were investigated. The Py–PES nanofibrous film, prepared under the optimum conditions and measured at pyrene excimer peak, shows good sensitivity to nitro-based explosives in aqueous phase, especially for PA with a LOD as low as 23 nM. The calculated K_{SV} values are 1.263×10^6 M^{-1} for PA (0–1 μM), 1.80×10^5 M^{-1} for TNT, 7.52×10^4 M^{-1} for DNT, 3.26×10^4 M^{-1} for RDX. In addition, pyrene monomer peak was also quenched by explosives. The observed nonlinearity of the Stern–Volmer plots indicates that both energy transfer and electron transfer mechanisms are responsible for the observed fluorescence quenching. Fluorescence lifetime measurements further reveal that the static quenching is dominant for the Py–PES nanofibrous film through formation of nonfluorescent complex between the fluorophore and electron-deficient explosives. Furthermore, common interferents have insignificant effect on the emission of the Py–PES nanofibrous film in aqueous phase, and the sensing film can be reused by simply washing with water. These features indicate that pyrene doped PES fluorescent sensors hold great promise in aqueous explosives detection due to its high sensitivity, good selectivity, cost effectiveness, and reusability.

ASSOCIATED CONTENT

Supporting Information

SEM images, quenching performance, pyrene excimer formation, absorption spectra of films, pyrene leaching studies in aqueous solution, tables of solution viscosities, fitting

DOI: 10.1021/acsami.5b03655
ACS Appl. Mater. Interfaces 2015, 7, 13189–13197

parameters for Stern−Volmer plots, molecular orbitals of compounds, and schematic illustration of photoinduced electron transfer mechanism. The Supporting Information is available free of charge on the ACS Publications website at DOI: 10.1021/acsami.5b03655.

AUTHOR INFORMATION

Corresponding Author

*E-mail: ylei@engr.uconn.edu. Phone: +1 (860) 486-4554. Fax: +1 (860) 486-2959.

Notes

The authors declare no competing financial interest.

ACKNOWLEDGMENTS

We are grateful for the financial support from National Science Foundation (NSF), the University of Connecticut Prototype Fund, and the University of Connecticut Startup Fund (J.Z.).

REFERENCES

(1) Lan, A.; Li, K.; Wu, H.; Olson, D. H.; Emge, T. J.; Ki, W.; Hong, M.; Li, J. A Luminescent Microporous Metal−Organic Framework for the Fast and Reversible Detection of High Explosives. *Angew. Chem., Int. Ed.* **2009**, *48*, 2334−2338.

(2) Salinas, Y.; Martinez-Manez, R.; Marcos, M. D.; Sancenon, F.; Costero, A. M.; Parra, M.; Gil, S. Optical Chemosensors and Reagents To Detect Explosives. *Chem. Soc. Rev.* **2012**, *41*, 1261−1296.

(3) Che, Y.; Gross, D. E.; Huang, H.; Yang, D.; Yang, X.; Discekici, E.; Xue, Z.; Zhao, H.; Moore, J. S.; Zang, L. Diffusion-Controlled Detection of Trinitrotoluene: Interior Nanoporous Structure and Low Highest Occupied Molecular Orbital Level of Building Blocks Enhance Selectivity and Sensitivity. *J. Am. Chem. Soc.* **2012**, *134*, 4978−4982.

(4) Nagarkar, S. S.; Joarder, B.; Chaudhari, A. K.; Mukherjee, S.; Ghosh, S. K. Highly Selective Detection of Nitro Explosives by a Luminescent Metal−Organic Framework. *Angew. Chem., Int. Ed.* **2013**, *52*, 2881−2885.

(5) Demirel, G. B.; Daglar, B.; Bayindir, M. Extremely Fast and Highly Selective Detection of Nitroaromatic Explosive Vapours Using Fluorescent Polymer Thin Films. *Chem. Commun.* **2013**, *49*, 6140−6142.

(6) Sun, X.; Brückner, C.; Nieh, M.-P.; Lei, Y. A Fluorescent Polymer Film with Self-Assembled Three-Dimensionally Ordered Nanopores: Preparation, Characterization and Its Application for Explosives Detection. *J. Mater. Chem. A* **2014**, *2*, 14613−14621.

(7) Toal, S. J.; Trogler, W. C. Polymer Sensors for Nitroaromatic Explosives Detection. *J. Mater. Chem.* **2006**, *16*, 2871−2883.

(8) Thomas, S. W.; Joly, G. D.; Swager, T. M. Chemical Sensors Based on Amplifying Fluorescent Conjugated Polymers. *Chem. Rev.* **2007**, *107*, 1339−1386.

(9) Rochat, S.; Swager, T. M. Conjugated Amplifying Polymers for Optical Sensing Applications. *ACS Appl. Mater. Interfaces* **2013**, *5*, 4488−4502.

(10) Swager, T. M. The Molecular Wire Approach to Sensory Signal Amplification. *Acc. Chem. Res.* **1998**, *31*, 201−207.

(11) Zhao, D.; Swager, T. M. Sensory Responses in Solution vs Solid State: A Fluorescence Quenching Study of Poly(iptycenebutadiynylene)s. *Macromolecules* **2005**, *38*, 9377−9384.

(12) Sanchez, J. C.; DiPasquale, A. G.; Rheingold, A. L.; Trogler, W. C. Synthesis, Luminescence Properties, and Explosives Sensing with 1,1-Tetraphenylsilole- and 1,1-Silafluorene-vinylene Polymers. *Chem. Mater.* **2007**, *19*, 6459−6470.

(13) Zang, L.; Che, Y.; Moore, J. S. One-Dimensional Self-Assembly of Planar π-Conjugated Molecules: Adaptable Building Blocks for Organic Nanodevices. *Acc. Chem. Res.* **2008**, *41*, 1596−1608.

(14) Kartha, K. K.; Babu, S. S.; Srinivasan, S.; Ajayaghosh, A. Attogram Sensing of Trinitrotoluene with a Self-Assembled Molecular Gelator. *J. Am. Chem. Soc.* **2012**, *134*, 4834−4841.

(15) Kartha, K. K.; Sandeep, A.; Praveen, V. K.; Ajayaghosh, A. Detection of Nitroaromatic Explosives with Fluorescent Molecular Assemblies and π-Gels. *Chem. Rec.* **2015**, *15*, 252−265.

(16) Kartha, K. K.; Sandeep, A.; Nair, V. C.; Takeuchi, M.; Ajayaghosh, A. A Carbazole-Fluorene Molecular Hybrid for Quantitative Detection of TNT Using a Combined Fluorescence and Quartz Crystal Microbalance Method. *Phys. Chem. Chem. Phys.* **2014**, *16*, 18896−18901.

(17) Wang, X.; Guo, Y.; Li, D.; Chen, H.; Sun, R.-c. Fluorescent Amphiphilic Cellulose Nanoaggregates for Sensing Trace Explosives in Aqueous Solution. *Chem. Commun.* **2012**, *48*, 5569−5571.

(18) Zhang, S.; Ding, L.; Lü, F.; Liu, T.; Fang, Y. Fluorescent Film Sensors Based on SAMs of Pyrene Derivatives for Detecting Nitroaromatics in Aqueous Solutions. *Spectrochim. Acta, Part A* **2012**, *97*, 31−37.

(19) Du, H.; He, G.; Liu, T.; Ding, L.; Fang, Y. Preparation of Pyrene-Functionalized Fluorescent Film with a Benzene Ring in Spacer and Sensitive Detection to Picric Acid in Aqueous Phase. *J. Photochem. Photobiol., A* **2011**, *217*, 356−362.

(20) Toal, S. J.; Magde, D.; Trogler, W. C. Luminescent Oligo(tetraphenyl)silole Nanoparticles as Chemical Sensors for Aqueous TNT. *Chem. Commun.* **2005**, 5465−5467.

(21) He, G.; Yan, N.; Yang, J.; Wang, H.; Ding, L.; Yin, S.; Fang, Y. Pyrene-Containing Conjugated Polymer-Based Fluorescent Films for Highly Sensitive and Selective Sensing of TNT in Aqueous Medium. *Macromolecules* **2011**, *44*, 4759−4766.

(22) Wang, Y.; La, A.; Ding, Y.; Liu, Y.; Lei, Y. Novel Signal-Amplifying Fluorescent Nanofibers for Naked-Eye-Based Ultrasensitive Detection of Buried Explosives and Explosive Vapors. *Adv. Funct. Mater.* **2012**, *22*, 3547−3555.

(23) Sun, X.; Liu, Y.; Mopidevi, S.; Meng, Y.; Huang, F.; Parisi, J.; Nieh, M.-P.; Cornelius, C.; Suib, S. L.; Lei, Y. Super-Hydrophobic "Smart" Sand for Buried Explosive Detection. *Sens. Actuators, B* **2014**, *195*, 52−57.

(24) Greiner, A.; Wendorff, J. H. Electrospinning: A Fascinating Method for the Preparation of Ultrathin Fibers. *Angew. Chem., Int. Ed.* **2007**, *46*, 5670−5703.

(25) Bhardwaj, N.; Kundu, S. C. Electrospinning: A Fascinating Fiber Fabrication Technique. *Biotechnol. Adv.* **2010**, *28*, 325−347.

(26) Wang, X.; Drew, C.; Lee, S.-H.; Senecal, K. J.; Kumar, J.; Samuelson, L. A. Electrospun Nanofibrous Membranes for Highly Sensitive Optical Sensors. *Nano Lett.* **2002**, *2*, 1273−1275.

(27) Long, Y.; Chen, H.; Yang, Y.; Wang, H.; Yang, Y.; Li, N.; Li, K.; Pei, J.; Liu, F. Electrospun Nanofibrous Film Doped with a Conjugated Polymer for DNT Fluorescence Sensor. *Macromolecules* **2009**, *42*, 6501−6509.

(28) Tang, Z.; Qiu, C.; McCutcheon, J. R.; Yoon, K.; Ma, H.; Fang, D.; Lee, E.; Kopp, C.; Hsiao, B. S.; Chu, B. Design and Fabrication of Electrospun Polyethersulfone Nanofibrous Scaffold for High-Flux Nanofiltration Membranes. *J. Polym. Sci., Part B: Polym. Phys.* **2009**, *47*, 2288−2300.

(29) Ding, L.; Liu, Y.; Cao, Y.; Wang, L.; Xin, Y.; Fang, Y. A Single Fluorescent Self-Assembled Monolayer Film Sensor with Discriminatory Power. *J. Mater. Chem.* **2012**, *22*, 11574−11582.

(30) Liu, T.; Ding, L.; Zhao, K.; Wang, W.; Fang, Y. Single-Layer Assembly of Pyrene End-Capped Terthiophene and Its Sensing Performances to Nitroaromatic Explosives. *J. Mater. Chem.* **2012**, *22*, 1069−1077.

(31) Liao, Y. Z.; Strong, V.; Wang, Y.; Li, X.-G.; Wang, X.; Kaner, R. B. Oligotriphenylene Nanofiber Sensors for Detection of Nitro-Based Explosives. *Adv. Funct. Mater.* **2012**, *22*, 726−735.

(32) Fong, H.; Chun, I.; Reneker, D. Beaded Nanofibers Formed During Electrospinning. *Polymer* **1999**, *40*, 4585−4592.

(33) Nirmala, R.; Panth, H. R.; Yi, C.; Nam, K. T.; Park, S.-J.; Kim, H. Y.; Navamathavan, R. Effect of Solvents on High Aspect Ratio Polyamide-6 Nanofibers via Electrospinning. *Macromol. Res.* **2010**, *18*, 759−765.

(34) Luo, C.; Nangrejo, M.; Edirisinghe, M. A Novel Method of Selecting Solvents for Polymer Electrospinning. *Polymer* **2010**, *51*, 1654−1662.
(35) Yuan, X.; Zhang, Y.; Dong, C.; Sheng, J. Morphology of Ultrafine Polysulfone Fibers Prepared by Electrospinning. *Polym. Int.* **2004**, *53*, 1704−1710.
(36) Wei, W.; Yeh, J.-T.; Li, P.; Li, M.-R.; Li, W.; Wang, X.-L. Effect of Nonsolvent on Morphologies of Polyamide 6 Electrospun Fibers. *J. Appl. Polym. Sci.* **2010**, *118*, 3005−3012.
(37) Qi, Z.; Yu, H.; Chen, Y.; Zhu, M. Highly Porous Fibers Prepared by Electrospinning a Ternary System of Nonsolvent/Solvent/Poly(L-lactic acid). *Mater. Lett.* **2009**, *63*, 415−418.
(38) Antoniou, E.; Alexandridis, P. Polymer Conformation in Mixed Aqueous-Polar Organic Solvents. *Eur. Polym. J.* **2010**, *46*, 324−335.
(39) Choktaweesap, N.; Arayanarakul, K.; Aht-Ong, D.; Meechaisue, C.; Supaphol, P. Electrospun Gelatin Fibers: Effect of Solvent System on Morphology and Fiber Diameters. *Polym. J.* **2007**, *39*, 622−631.
(40) Chen, H.-C.; Tsai, C.-H.; Yang, M.-C. Mechanical Properties and Biocompatibility of Electrospun Polylactide/Poly(vinylidene fluoride) Mats. *J. Polym. Res.* **2011**, *18*, 319−327.
(41) Yang, T.; Wu, D.; Lu, L.; Zhou, W.; Zhang, M. Electrospinning of Polylactide and Its Composites with Carbon Nanotubes. *Polym. Compos.* **2011**, *32*, 1280−1288.
(42) Beyazkilic, P.; Yildirim, A.; Bayindir, M. Formation of Pyrene Excimers in Mesoporous Ormosil Thin Films for Visual Detection of Nitro-Explosives. *ACS Appl. Mater. Interfaces* **2014**, *6*, 4997−5004.
(43) Sun, X.; Ma, X.; Kumar, C. V.; Lei, Y. Protein-Based Sensitive, Selective and Rapid Fluorescence Detection of Picric Acid in Aqueous Media. *Anal. Methods* **2014**, *6*, 8464−8468.
(44) Venkatramaiah, N.; Kumar, S.; Patil, S. Fluoranthene Based Fluorescent Chemosensors for Detection of Explosive Nitroaromatics. *Chem. Commun.* **2012**, *48*, 5007−5009.
(45) Focsaneanu, K.-S.; Scaiano, J. Potential Analytical Applications of Differential Fluorescence Quenching: Pyrene Monomer and Excimer Emissions as Sensors for Electron Deficient Molecules. *Photochem. Photobiol. Sci.* **2005**, *4*, 817−821.
(46) Agudelo-Morales, C. E.; Galian, R. E.; Pérez-Prieto, J. Pyrene-Functionalized Nanoparticles: Two Independent Sensors, the Excimer and the Monomer. *Anal. Chem.* **2012**, *84*, 8083−8087.
(47) Lakowicz, J. R. *Principles of Fluorescence Spectroscopy*, 3rd ed.; Springer: Singapore, 2006.
(48) Eftink, M. R.; Selvidge, L. A. Fluorescence Quenching of Liver Alcohol Dehydrogenase by Acrylamide. *Biochemistry* **1982**, *21*, 117−125.
(49) Olley, D. A.; Wren, E. J.; Vamvounis, G.; Fernee, M. J.; Wang, X.; Burn, P. L.; Meredith, P.; Shaw, P. E. Explosive Sensing with Fluorescent Dendrimers: The Role of Collisional Quenching. *Chem. Mater.* **2011**, *23*, 789−794.
(50) Bhalla, V.; Gupta, A.; Kumar, M.; Rao, D. S. S.; Prasad, S. K. Self-Assembled Pentacenequinone Derivative for Trace Detection of Picric Acid. *ACS Appl. Mater. Interfaces* **2013**, *5*, 672−679.
(51) Fan, L.; Hu, Y.; Wang, X.; Zhang, L.; Li, F.; Han, D.; Li, Z.; Zhang, Q.; Wang, Z.; Niu, L. Fluorescence Resonance Energy Transfer Quenching at the Surface of Graphene Quantum Dots for Ultra-sensitive Detection of TNT. *Talanta* **2012**, *101*, 192−197.
(52) Dalapati, S.; Jin, S.; Gao, J.; Xu, Y.; Nagai, A.; Jiang, D. An Azine-Linked Covalent Organic Framework. *J. Am. Chem. Soc.* **2013**, *135*, 17310−17313.

DOI: 10.1021/acsami.5b03655
ACS Appl. Mater. Interfaces 2015, 7, 13189−13197